An investigation on stability of laser hybrid arc welding

Moradi, M., Ghoreishi, M., Frostevarg, J. & Kaplan, A. F. H.

Original citation & hyperlink:
Moradi, M, Ghoreishi, M, Frostevarg, J & Kaplan, AFH 2013, 'An investigation on stability of laser hybrid arc welding', Optics and Lasers in Engineering, vol. 51, no. 4, pp. 481-487.
https://dx.doi.org/10.1016/j.optlaseng.2012.10.016

DOI 10.1016/j.optlaseng.2012.10.016
ISSN 0143-8166

Publisher: Elsevier

An investigation on stability of laser hybrid arc welding

Mahmoud Moradi[1, 2], Majid Ghoreishi[1], Jan Frostevarg[2], Alexander F.H. Kaplan[2]

[1]Faculty of Mechanical Engineering, K.N. Toosi University of Technology, P. O. Box 1999143344, Tehran, Iran

[2] Department of Engineering Sciences and Mathematics, Luleå University of Technology, S-971 87 Luleå, Sweden

Abstract

The stability of the weld surface quality resulting from laser-arc hybrid welding of 4 mm thick steel was studied. The trends of stability in terms of top weld width variation were estimated by using design of experiments, where different types of unstable welds were distinguished. High speed imaging of the process supported the interpretation of the trends. High arc voltage and short distance laser-arc has destabilized the process. For a stable process the applied spray mode has caused a short arc and symmetric central drop transfer while for high voltage the arc became long and wide and the drops travelled sideward. The potential and limits of the design of experiments method for such kinds of applications were discussed.

Keywords: laser hybrid arc welding, welding stability, Design of Experiments, high speed imaging

1. Introduction

Laser hybrid arc welding, LHAW, [1] first published in 1979 [2], combines an electric arc with a laser beam. When two techniques are coupled, the number of process parameters is large and therefore difficult to optimize in order to achieve the desired weld quality and speed. Deeper weld penetration, less deformation, high welding speed, the ability to bridge relatively large gaps, capability of welding highly reflective materials and improvement of the arc stability can be advantages of laser hybrid arc welding [3, 4].

Performing experimental work empirically by trial-and-error is often done but time consuming [5, 6]. The use of the Design-of-Experiments method, DOE, has grown recently in different applications [7-10]. The advantage of the Response Surface Methodology, RSM, as one of the DOE-approaches [7, 11] is the proper reduction in the number of experiments, through achieving a logical relationship between the input and output parameters by considering interaction effects and developing mathematical functions. With this method, laser hybrid arc welding was studied with respect to undercut defects for steel surfaces [1]. Moradi and Ghoreishi,[8] have developed mathematical models to study the effect of the laser welding parameters of Ni-Base Super Alloy Rene80 on weld-bead profiles using RSM. Karlsson et al [12] and Norman et al [13] observed the mechanisms causing two kinds of undercut during fiber laser hybrid arc welding by high speed imaging and SEM along with new documentation methods like the Matrix Flow Chart, MFC, and the Bifurcation Flow Chart, BFC. Liming liu et al. [14]improved laser keyhole formation with the assistance of arc plasma in the hybrid welding process of magnesium alloy. Cerit et al [15] surveyed stress concentration effects of undercut defects and reinforcement of metals in butt welded joints using the Finite Element Method. For MIG-CO_2 laser hybrid arc welding of AlMg alloy the DOE method was used [16]. Jun Yan et al. [17] Studied the microstructure and mechanical properties of 304 stainless steel joints by TIG, laser and laser-TIG hybrid welding. The weld penetration was the only design output variable. Moradi et al [18] modeled and optimized the weld bead profile of laser-TIG hybrid welding of stainless steel by using the RSM. Liu and Chen [19], investigated on the interactions between laser and arc plasma during laser–arc hybrid welding on magnesium alloy AZ31B using the spectral diagnose technique.

Very common for LHAW is to operate the MAG-arc in the pulsed mode,[12, 13] where one drop per pulse is detached and transferred in a controlled manner. For the pulsed mode, the impact of the geometrical edge properties of a butt joint were studied by surface scanning and high speed imaging, to identify the range of operating windows as well as their limits of stability [20] For pulsed mode LHAW, the stability of the arc and of the resulting weld was studied for different wire chemistry, altering the Alkali metal content, by assessing the weld surface appearance (spatter), by measuring the arc width and length variations in high speed imaging and by evaluating variations in the voltage signal, particularly short-circuiting [21]. It was confirmed that different Alkali metals have different impact on the arc stability. In particular, Na and Li were favored compared to K. In arc welding, different techniques like the spray mode [22] or globular drop transfer are also common. A recently developed (pulsed) arc technique is Cold Metal Transfer, CMT,[23] where instead of constant wire feeding the wire is periodically pulled back. In the present study the spray mode will be studied, i.e. the arc is operated at constant voltage.

The purpose of the present study is to analyze by the aid of DOE the stability of the resulting weld surface appearance and in turn of the welding process for fiber laser-MAG hybrid welding of stainless steel. The three process parameters varied for the statistical analysis are voltage, distance laser-arc and laser beam power. The interpretation of the DOE-results is supported by high speed imaging of the welding process.

2. Methodological approach

2.1. Experimental set-up

In this study, 4 mm thick stainless steel 1.4418 was welded bead-on-plate (BOP, representing a zero gap butt joint), with Lincoln SupraMIG Ultra as the filler material. The chemical composition of the material and wire is given in Table 1. The BOP-samples had a length of 70 mm and a width of 120 mm.

Table 1: Chemical composition (wt.-%) of the sheet material (upper) and the wire (lower)

	Fe	C	Si	Mn	Cr	Ni	Mo	Cu	W	V
SS 1.4418	Bal.	0.037	0.21	0.72	15.91	4.89	0.86	0.22	0.15	0.11
Lincoln SupraMIG Ultra	Bal.	0.08	0.85	1.7						

A 15 kW Yb:fiber laser (IPG, YLR-15000) with a fiber diameter of 200 µm was operated in a range of 3.5-5.5 kW (continuous wave). Optics with a focal length of 300 mm created a focus diameter of 400 µm. The laser was combined with a Metal Active Gas (MAG, gas mixture 92% Ar, 8% CO_2) arc, operated with constant voltage in the range of 20-40 V in the spray mode, leading, at an angle of 57° from the surface. The distance laser-arc was varied between 0 and 4 mm. The fixed process parameters are presented in Table 3. The three parameters that were varied as the input properties of the DOE-method are laser power P, arc voltage U and distance laser-arc d_{LA}.

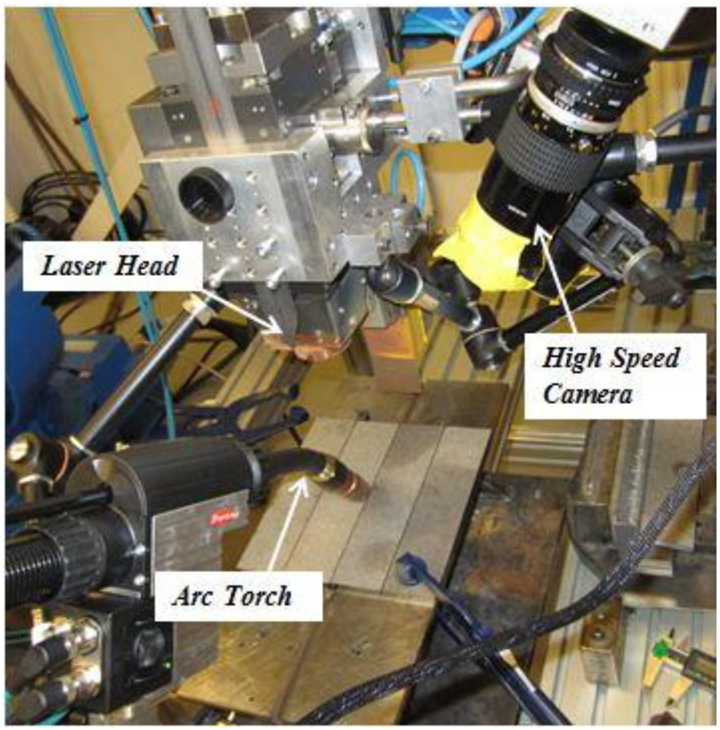

Fig. 1: Experimental set-up of LHAW

Table 2: Fixed LAHW process parameters

Parameter	Value
Focal plane position	-2 mm
Shielding gas pressure	20 l/min
Wire feeding rate	6 m/min
Welding speed	3 m/min
Wire diameter	1.2 mm
Torch angle (from the surface)	57º
Laser tilting angle	7º
Wire stickout length	20 mm

In this study, from each welded sample a photo of the weld top surface appearance was taken, as shown in Fig 2(a). From the weld surface geometry the stability was expressed through the following definition; The widest and the narrowest part of the weld surface were measured and the absolute difference expresses the variation of the weld surface width, i.e. higher difference corresponds to lower stability. For some samples the character of the weld appearance changed along the weld; Therefore, along the 70 mm long weld it was divided into a 20 mm long upper part U and a lower part L, see Fig. 2. This definition excludes also the weld start and stop regions. Consequently, two weld width variation values are obtained, for the upper and lower part:

$$\Delta W_U = W_{Umax} - W_{Umin} \quad (1)$$

$$\Delta W_L = W_{Lmax} - W_{Lmin} \quad (2)$$

For each sample, finally the level of instability (the lower ΔW the more stable the weld) is expressed through the larger of the two values:

$$\Delta W = \text{Max}\ \{\Delta W_U, \Delta W_L\} \quad (3)$$

This value is the response property for the design of experiments study. Owing to its ease of use this definition was preferred to more sophisticated stability calculation methods like the standard deviation of the weld width or its moving average.

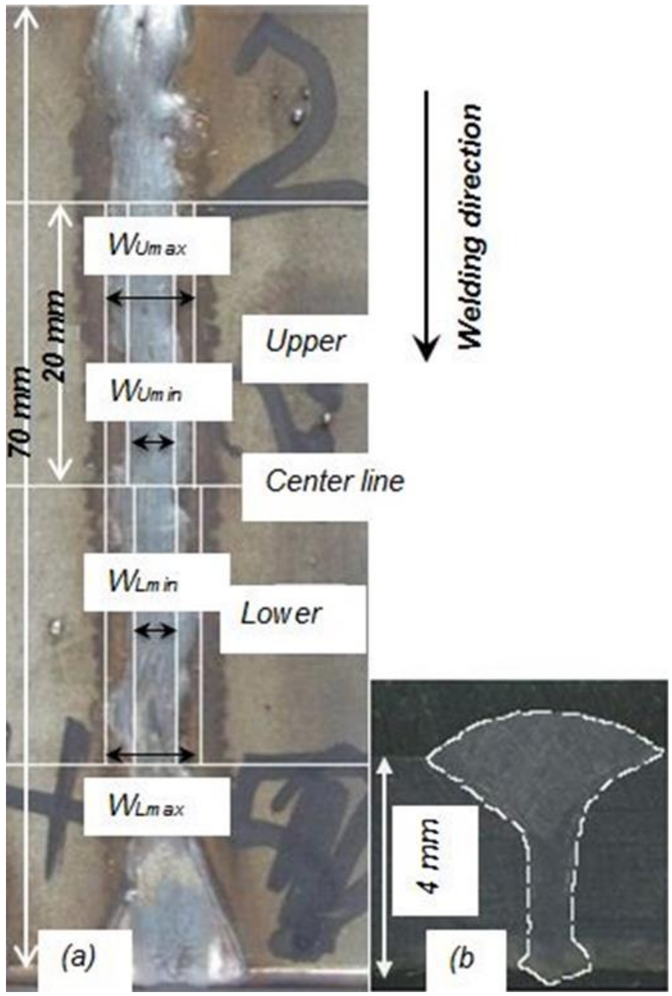

Fig 2: (a) Weld top surface appearance and the definition of stability through upper and lower weld width variation, (b) typical laser hybrid arc weld cross section

2.2 Design-of-Experiment method

The Design-of-Experiment method, DOE, was applied in order to systematically visualize and analyze the trends of the stability as a function of three selected parameters. The process of DOE-modelling is generally influenced by the method which has been chosen for conducting and designing the experiments. The Response Surface Methodology, RSM, is one of these methods, which is a set of mathematical and statistical techniques that is useful for modelling and predicting the desired response [15, 16]. Furthermore, the RSM specifies the relationships between one or more measured responses and the essential controllable input factors [18]. When all independent variables x are measurable and experiments can be repeated with negligible errors, the RSM can be defined as follows:

$$Y = f(x_1, x_2, x_3, \ldots, x_k), \quad (4)$$

where k is the number of independent variables. Finding a function to relate the independent variables to their responses is essential. In general, a second-order (quadratic) polynomial is used in the RSM to precise the model and responses as follows:

$$y = \beta_0 + \sum_{i=1}^{k} \beta_i x_i + \sum_{i=1}^{k} \beta_{ii} x_i^2 + \sum_i \sum_j \beta_{ij} x_i x_j + \varepsilon \quad (5)$$

where β_0 is the constant value or intercept, β_i the linear coefficient, β_{ii} the quadratic coefficient, β_{ij} the interaction coefficient and ε is the random error of the developed regression [8].

Linear and second order polynomials were found best to fit to the experimental data, using the sequential F-test and T-test. Lack-of-fit test and other adequate measures were also employed to validate the accuracy of the developed regression equations. Curvatures or 3D-plots on the developed response surfaces show that the parameter ranges of a process were selected correctly and that optimum setting would exist in the considered parameters space.

In the present study, the experiments were designed based on a Central Composite Design (CCD) five-level RSM design [5]. The commercial DOE software code Minitab was applied. Laser power P (3.5-5.5 kW), arc voltage U (20-40 V) and distance laser-arc d_{LA} (0-4 mm) were selected as the three process-independent input variables. Table 3 shows the process input variables and the five experimental design levels (from -2 to +2) illustrated with coded and actual values while Table 4 shows the designed matrix with the measured values of the responses, namely the stability expressed through the weld width variation ΔW. The experimental design encompasses 17 experiments which include eight experiments as factorial points in the cubic vertex, six experiments as axial points and three experiments in the cubic centre as centre point experiments. In Table 4 a subjective rating of the appearance of weld surface stability is also added, divided into upper U and lower L weld section. Five categories were distinguished: A stable weld of low width variation, B moderate symmetric width oscillation, C moderate alternating or wavy width variation, D strong symmetric width variation, E strong asymmetric or irregular width variation

Table 3. The three independent LHAW process parameters and their five values, related to the five design levels (-2 to +2)

Parameters	Notation	Unit	-2	-1	0	1	2
Laser power	P	[kW]	3.5	4	4.5	5	5.5
Voltage	U	[V]	20	25	30	35	40
Distance	d_{LA}	[mm]	0	1	2	3	4

Table 4. Design matrix, comprising the 17 experiments, expressed by the three input process parameters as design levels and the weld width variation as the output response

Experiment no.	Laser power [-]	Arc voltage [-]	Distance laser-arc [-]	LHAW width variation ΔW [mm]	Stability rating U/L [A-E]
1	0	0	0	3.68	B/B
2	1	1	1	3.80	B/B
3	0	0	0	4.71	B/B
4	1	1	-1	7.60	B/D
5	2	0	0	2.26	A/A
6	0	0	0	3.88	B/B
7	-1	-1	-1	2.33	A/B
8	0	2	0	10.22	E/E
9	1	-1	-1	2.06	A/A
10	0	0	2	2.45	A/B
11	-1	-1	1	2.61	A/A
12	1	-1	1	2.35	A/A
13	0	-2	0	4.66	D/D
14	-1	1	1	8.71	E/E
15	-2	0	0	3.48	A/B
16	0	0	-2	5.05	C/C
17	-1	1	-1	9.64	E/E

2.3. High speed imaging

The 17 experiments were accompanied by high speed imaging of the process from the top to obtain additional information on the stability of the weld pool, keyhole, electric arc and drop transfer. During the last two decades high speed imaging of arc welding, laser welding and LHAW became usual to observe the process physics. The process is usually illuminated by an additional laser beam or by another light source, then by a narrow band filter eliminating most of the process light. While frame rates of 1000-20 000 fps became usual, in the present study a camera with a maximum frame rate of 180 000 fps was used. This work presents images taken by a Photron SA1 (San Diego, California) high-speed camera with a Micro-Nikkon 105 mm lens, at 180 000 frames per second with an exposure time of 370 ns. The image size was 128×128 pixels with 12 bit pixel depth. A fiber-guided pulsed diode laser (Cavitar, peak power 500 W) with a wavelength of 808 nm was illuminating the work piece surface, correspondingly narrow band pass-filtered by the camera objective. The experimental employment of the camera is shown in Fig. 1. The experiments involved a moving laser beam and camera by a robot, and a stationary work piece. The camera (and the illumination) was arranged to observe the process from the side, at a tilting angle of about 45º, capturing images as explained in Fig. 3.

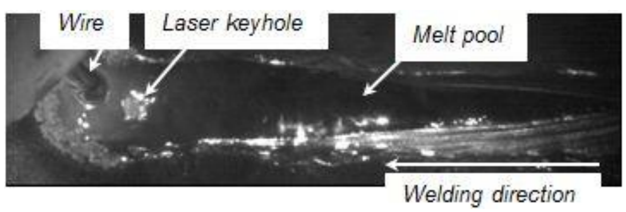

Fig. 3: Typical high speed image of the LHAW process (the wire diameter is 1.2mm)

3. Results and discussion

The 17 hybrid welds were carried out as planned for the design of experiments. Of the 17 weld surface appearances, nine characteristic samples are shown in Fig. 4. The photos are arranged as top view on the DOE plane where voltage U and distance laser-arc d_{LA} are varied, in the non-dimensional units of the DoE, i.e. from -2 to +2 according to the design matrix, see Table 4. For the power level a representative selection was made, see Table 4.

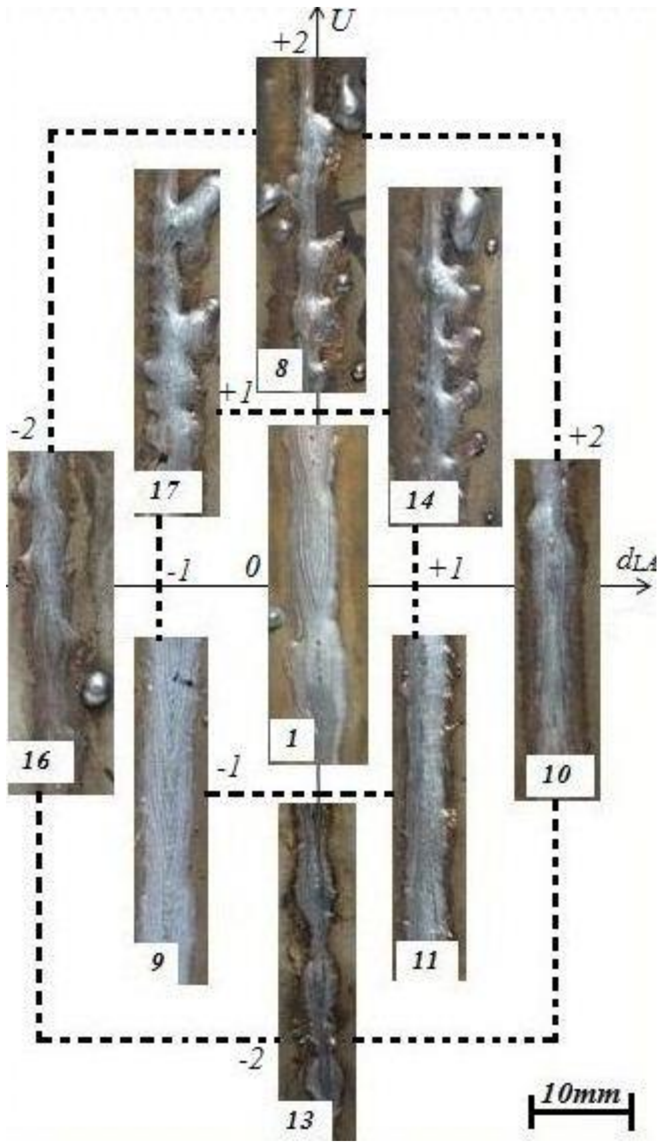

Fig. 4: Effect of the input parameter variations arc voltage U and distance laser-arc d_{LA} (design levels -2 to +2) on the weld top surface appearance (sample no. inserted), expressing the stability

As can be seen in Fig. 4, very high voltage of the spray arc strongly destabilizes the weld. Very low voltage, sample no. 13, also increased the weld width variation, in a symmetric oscillating manner. Very short distance laser-arc, sample no. 16, showed weld width variation in a wavy appearance. High stability was achieved in a wide range of parameters, preferably for moderate voltage. See also Table 4 for rating of the weld stability, classified A-E, separately for the respective upper and lower weld section U,L. The measured maximum weld width variation ΔW was listed in Tab. 4 for the 17 samples. For these response values the design of experiment analysis was then carried out through the Minitab software. A polynomial full quadratic model was used in this analysis. According to the results of an analysis of variance runs on the weld width variation ΔW, see Table 5, all parameters are significant. This is determined by sufficient low P-values below 0.08 in Table 5.

Table 5: Modified DOE analysis of variance on ΔW, resulting from DOE of the 17 LHAW experiments through the Minitab software, as the numerical base for the formula describing the parameter dependencies

Source of variation	Sum of squares	Degree of freedom	Mean squares	T value	F value	P value
Regression	101.683	5	20.3366	10.401	14.51	0.000
P	6.162	1	6.162	-2.097	4.40	0.060
U	62.146	1	62.146	6.660	44.35	0.000
d_{LA}	5.477	1	5.477	-1.977	3.91	0.074
U×U	22.742	1	22.742	4.029	16.23	0.002
P×U	5.157	1	5.157	-1.918	3.68	0.081
Residual Error	15.412	11	1.4011			
Pure Error	0.594	2	0.2968			
Lack-of-Fit	14.819	9	1.6465	-	5.55	0.162
Total	117.095	16				
R-Sq =86.84%	R-Sq (adj)=80.85%					

Among quadratic terms, the quadratic term of voltage has a significant effect while other quadratic terms are insignificant. Likewise, only the quadratic effect of laser power and arc voltage is significant. The analysis of variance (ANOVA) table of the weld width variation ΔW indicates that the regression model output fits to the weld penetration with a good estimation. Meanwhile the Lack-of fit has been shown to be insignificant. It should be noticed that in the ANOVA analysis the best situation occurs when the regression model is significant and Lack-of fit is insignificant at the same time. From the DOE analysis the Minitab software elaborated the following regression formula for the LHAW stability as a function of the three varied process parameters, $\Delta W(U,d_{LA},P)$:

$$\Delta W = 3.78 - 0.62P + 1.97U - 0.58\, d_{LA} + 0.95U^2 - 0.8\, PU \qquad (6)$$

The corresponding dependency of the weld width variation ΔW on the three variables is visualized in Fig. 5.

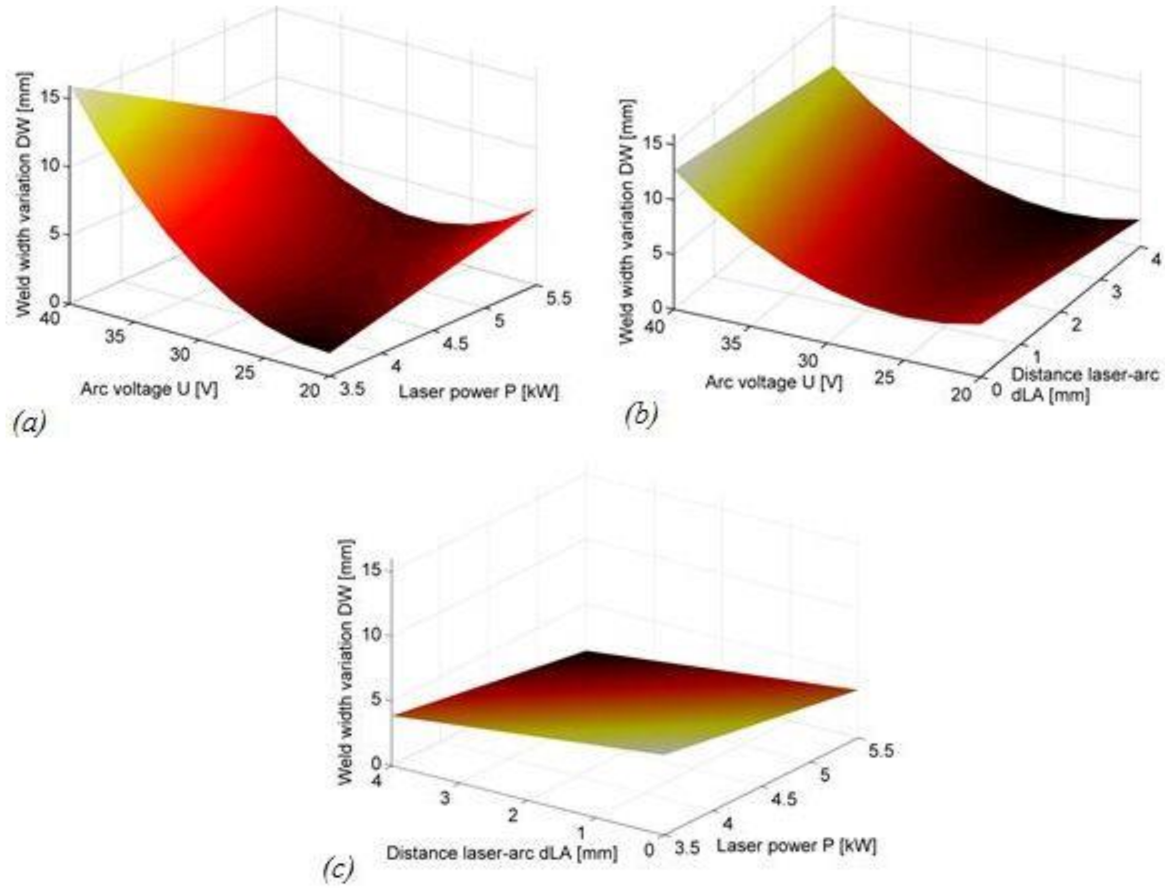

Fig. 5: Stability of LHAW expressed by low weld width variation ΔW from Design-of-Experiments analysis, visualized in dependence of two process parameters: (a) arc voltage and laser power, (b) arc voltage and distance laser-arc, (c) distance laser-arc and laser power

As can be seen, the weld becomes strongly unstable (high ΔW) for increasing voltage, as well confirmed by Fig. 4. This trend becomes also clear through the U-term in Eq. (3). The distance laser-arc and the laser power have a weaker, linear influence. However, it should be noted that the linear influence of the laser power even changes sign, see Fig. 5(a). The DOE method here demonstrates that it enables to generalize and visualize results and to predict trends, while the collection of single welding results gives only a discrete picture across the parameter field. Because the DOE-results were calculated from the 17 experiments by a commercial software code, Minitab, in which not all mathematical and numerical details are accessible, the resulting formula, Eq. (3), and its derivation cannot be tracked back to the 17 sample outputs in detail. This makes an interpretation and validation of the DOE results more difficult. However, in the present case, the DOE-results in Fig. 5 correlate very well with the surface appearances in Fig. 4.

For example the corners of the plots in Fig. 5 used to be less safe and exaggerated through the DOE, because they are more far away and less surrounded from data points.

Additional information was obtained by high speed imaging. Figure 6 shows sequences of the drop transfer from the wire to the surface for four different cases.

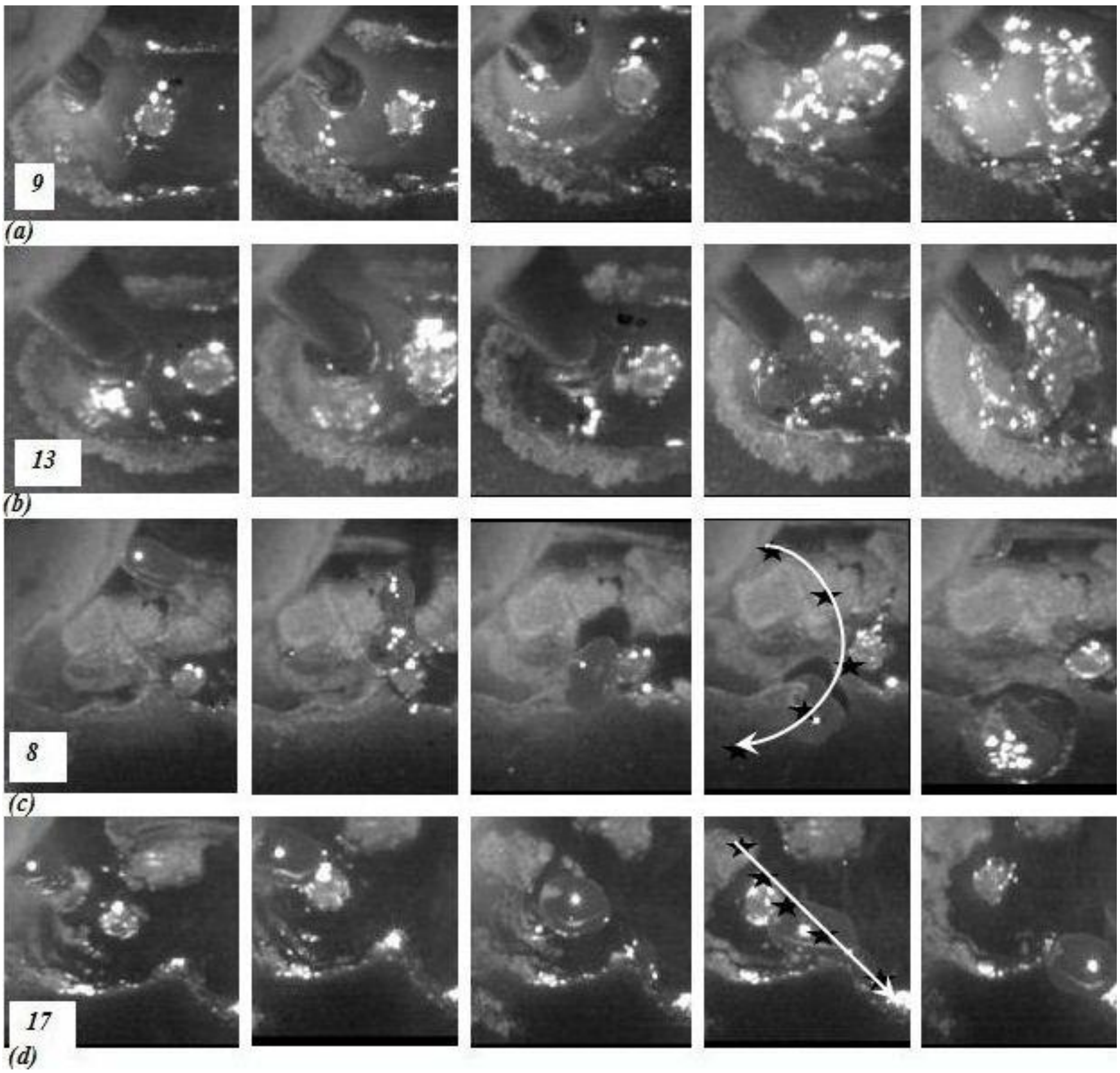

Fig 6: Sequences (time steps of 247 µs) of high speed images of the drop transfer during LHAW for four characteristic cases: (a) experiment no. 9, stable weld, (b) no. 13, symmetrically oscillating instability, (c) no. 8, strong asymmetric instability, (d) no. 17, strong asymmetric instability

For a weld of high quality, sample no. 9 in Fig.4, the arc length is short; see Fig. 6(a), and the drop transfer remains very central, symmetric and repeatable. The symmetric oscillation of the weld for sample no. 13 in Fig. 4, for which the drop transfer is shown in Fig. 6(b), can be explained by periodic accumulation of large drops before transfer and corresponding weld width variation. Laser driven narrow weld sections due to the delay of drop delivery are followed by sections filled by large grown drops. Due to the short distance laser-arc the drop interacted directly with the keyhole, causing additional flow disturbances. For high voltage, samples no. 13 and no. 17 in Fig. 4, the high instability of the process can be observed through drop trajectories that are strongly oriented sideward, as can be seen in Fig. 6(c) for a curved path and in Fig. 6(d) for a straight sideward path. Here the spray arc is very long and wide which facilitates redirection of the arc to one side and, owing to the magnetic forces, of the drop to the other side. The average drop transfer period for the spray mode was measured to be 17.4 ms, varying up to 30%. High speed imaging is a very powerful method to support and interpret DOE-analysis, as part of the trends can be well observed and explained.

4. Conclusion

From high speed imaging and DOE of laser hybrid arc welding the following conclusions can be drawn:

(i) High speed imaging of the welding process strongly supports the interpretation of the DOE-trends.

(ii) Increasing arc voltage strongly destabilizes the resulting weld surface because the spray arc becomes very long and wide and the drops travel sideward.

(iii) Short distance laser-arc as well as high laser power can also cause instabilities.

(iv) DOE turns out to be useful to visualize and generalize parameter trends, even for welding stability as a complex aspect, but it requires preparatory experiments for the parameters to be fixed; the commercial codes do not enable to track the calculated results back to the samples

References

1. *C. Bagger, F.O. Olsen., Review of laser hybrid welding. J. Laser Appl., 2005. 17: p. 2-14.*
2. *W.M. Steen, M.Eboo, Arc augmented laser welding. Metals Constr 1979. 7: p. 332-336.*
3. *M. Gao, X. Zeng, Q. Hu, Effects of gas shielding parameters on weld penetration of CO2 laser-TIG hybrid welding. Journal of Materials Processing Technology, 2007. 184(1-3): p. 177-183.*
4. *R. Poprawe, Laser Application Technology. 2011: springer.*
5. *D.C. Montgomery, Design and Analysis of Experiments. 2009, New York: John Wiley.*
6. *R.H. Myers, D.C. Montgomery., Response surface methodology: Process and product optimization using designed experiments. 1995, New York: Wiley.*
7. *K.Y. Benyounis, A.G. Olabi, M.S.J. Hashmi, Multi-response optimization of CO2 laser-welding process of austenitic stainless steel. Optics and Laser Technology 2008. 40(1): p. 76-87.*
8. *M.Moradi , M.Ghoreishi, Influences of laser welding parameters on the geometric profile of NI-base superalloy Rene 80 weld-bead. Int J Adv Manuf Technol, 2011. 55: p. 205–215.*
9. *M.Moradi , M.Ghoreishi, Laser welding process optimization using statistical design of experiments, in 18th Annual International Conference on Mechanical Engineering-ISME2010. 2010: Sharif University of Technology, Tehran, Iran.*
10. *M. Ghoreishi, J. Atkinson, A comparative experimental study of machining characteristics in vibratory, rotary and vibro-rotary electro-discharge machining. Jornal of Materials Processing Technology, 2002(120): p. 374-384.*
11. *A.I. Khuri, J.A. Cornel., Response Surfaces Design and Analysis. 1996, New York: Marcel Dekker.*
12. *J. Karlsson, P. Norman, A.F.H. Kaplan, P.Rubin, J.Lamas, A.Ya˜nez, Observation of the mechanisms causing two kinds of undercut during laser hybrid arc welding. Applied Surface Science, 2011. 257: p. 7501–7506.*
13. *P.M. Norman, J. Karlsson., A.F.H. Kaplan, Mechanisms Forming Undercuts during Laser Hybrid Arc Welding. Physics Procedia, 2011. 12: p. 201-207.*
14. *Liu, L. and X. Hao, Improvement of laser keyhole formation with the assistance of arc plasma in the hybrid welding process of magnesium alloy. Optics and Lasers in Engineering, 2009. 47(11): p. 1177-1182.*
15. *M. Cerit, O. Kokumer, K. Genel, Stress concentration effects of undercut defect and reinforcement metal in butt welded joint. Engineering Failure Analysis, 2010. 17: p. 571–578.*
16. *G. Casalino, Statistical analysis of MIG-laser CO2 hybrid welding of Al-Mg alloy. Journal of Materials Processing Technology, 2007. 191(1-3): p. 106-110.*
17. *Yan, J., M. Gao, and X. Zeng, Study on microstructure and mechanical properties of 304 stainless steel joints by TIG, laser and laser-TIG hybrid welding. Optics and Lasers in Engineering. 48(4): p. 512-517.*
18. *M.Moradi, M.Ghoreishi, M.J.Torkamany, J.Sabbaghzadeh, Modeling and optimization of Nd:YAG laser-TIG hybrid welding of stainless steel, Lasers in Engineering, (submitted) 2012.*
19. *Liu, L., Chen, M., Interactions between laser and arc plasma during laserarc hybrid welding of magnesium alloy. Optics and Lasers in Engineering, 2011. 49(9-10): p. 1224-1231.*
20. *J. Powell, J. Lamas, , J. Karlsson, P. Norman, A.F.H.Kaplan, A. Yanez, The sensitivity of hybrid laser welding to variations in workpiece position. Physics Procedia, 2011. 12, Part 1: p. 188-193.*
21. *P. Dyberg, A. F. H. Kaplan. On the influence of metal cored wire deposition on the hybrid welding process. in ICALEO. 2007. Orlando (FL).*
22. *G. Campana, A. Fortunato, A. Ascari. G. Tani, L. Tomesani, The influence of arc transfer mode in hybrid laser-MIG welding. Jornal of Materials Processing Technology, 2007. 191: p. 111-113.*
23. *C.G. Pickin, K. Young, Evaluation of cold metal transfer (CMT) process for welding aluminium alloy. Science and Technology of Welding & Joining, 2006. 11: p. 583-585.*